



23 **Abstract**

24 There are fundamental gaps in our understanding of the fates of microplastics in the ocean,  
25 which must be overcome if the severity of this pollution is to be fully assessed. The predominant  
26 pattern is high accumulation of microplastic in subtropical gyres. Using in situ measurements  
27 from the 7<sup>th</sup> Continent expedition in the North Atlantic subtropical gyre, data from satellite  
28 observations and models, we show how microplastic concentrations were up to 9.4 times higher  
29 in the anticyclonic eddy explored, compared to the cyclonic eddy. Satellite-observed  
30 chlorophyll-a was also more abundant inside the anticyclonic eddy (on average 30%). Although  
31 our sample size is small, this is the first suggestive evidence that mesoscale eddies might trap,  
32 concentrate and potentially transport microplastics. As eddies are known to congregate  
33 nutrients and organisms, this phenomenon should be considered with regards to the potential  
34 impact of plastic pollution on the ecosystem in the open ocean.

35

36 **Keywords**

37 Microplastic

38 North Atlantic subtropical gyre

39 Marine litter

40 Sea Level Anomalies

41 Mesoscale eddies

42 Satellite observations

43 Oceanic current models

44 **Highlights**

45 ● Discussion of the heterogeneity of surface plastic debris distribution at sea

46 ● In situ measurements and correlation with satellite observations

47 ● Rationalization by the local circulation in eddies

48

49

50

51

## 52 **Introduction**

53 Because of the durability of plastic and the constantly increasing inputs, plastic debris is  
54 accumulating in every environment. Plastic debris is found inland even in remote places like  
55 deserts (1). In aquatic environments, plastic has been found in rivers (2, 3), lakes (4, 5), bays  
56 (6), gulfs (7) and oceans (8). While the denser debris accumulates in rivers and estuarine sea  
57 floors (6), buoyant plastic mostly ends up in open oceans (9) where, after being transported  
58 over long distances, buoyant plastic debris tends to converge in subtropical gyres (10).

59 The impact of plastic pollution in the oceans affects the whole ecosystem. The direct effects are  
60 entanglement and ingestion. Plastic fragmentation results in a continuum of debris sizes (11),  
61 leading to microscopic and even nanometric fragments (12). Thus ingestion concerns both the  
62 larger animals, like cetaceans (13, 14), turtles (15), sea birds (16-18), and the smaller ones, like  
63 fishes (19); even zooplankton are concerned (20, 21). It has been demonstrated that plastic  
64 ingestion can significantly alter the feeding capacity and decrease the reproductive output of  
65 organisms (22). Another effect is the transportation of invasive species across oceans, which  
66 could potentially affect the equilibrium of ecosystems (23, 24). There are also toxic chemicals  
67 associated with plastic debris since the plastic contains additives, persistent organic pollutants  
68 and heavy metals (25). The transfer of these substances into the food web when plastic debris  
69 is ingested by animals has already been demonstrated for certain organisms (26-30).

70 Floating marine plastic debris converges in subtropical gyres (31-34). Some convergence areas  
71 have been much more surveyed than others, e.g. the western North Atlantic Ocean (31, 35) and  
72 the eastern North Pacific Ocean (33, 36). The southern hemisphere has been studied far less  
73 (32, 37). The vast majority of the sea surface has not been surveyed for plastic pollution and  
74 there is an evident lack of experimental measurements at sea. By means of circulation models,  
75 the weight of the global plastic debris floating at sea has been estimated at several hundred  
76 thousand metric tons (between 90 000 and 250 000 metric tons) (37, 38). These estimates

77 correspond to only 1% of the global plastic waste input into the ocean in 2010 (9). There is an  
78 obvious need to better understand where plastic debris is located at sea. This is a crucial step  
79 toward assessing the severity of the impact of plastic pollution on marine life.

80 Because ocean motion is complex and variable, it is difficult to determine precisely the  
81 boundaries of subtropical gyres (39) and we do not know, in real time, exactly where plastic  
82 particles are located and how they are distributed inside the accumulation areas. Simulations  
83 and models exist and are good indicators for a global approach (8, 40, 41). A recent article  
84 comparing existing models concluded that distributions of plastic within gyres were in relative  
85 agreement even if methods and inputs were different (38).

86 It has often been reported that the amount of plastic collected in trawls can show large  
87 variability, sometimes up to an order of magnitude within only a few tens of kilometers, but  
88 this has never been rationalized (38). Knowing that eddies (vortices of 50 to 200 km in diameter  
89 that are ubiquitous in the ocean) can trap and transport fluid parcels including nutrients,  
90 chlorophyll, and zooplankton (42-44), we set out to test the hypothesis that plastic distribution  
91 at the sea surface could be partly attributed to the presence of eddies. Traditionally, the  
92 paradigm is that anticyclonic eddies (clockwise in the Northern Hemisphere) capture material  
93 drifting at the surface, while cyclonic eddies (anticlockwise in the Northern Hemisphere) tend  
94 to expel material (44). However, the mechanisms are complex and some studies have shown  
95 that cyclonic eddies can also capture material very effectively (39, 45, 46).

96 Satellites providing near-surface information on ocean physics and biology are the only  
97 practical means of obtaining dense, global observations of the open ocean. But the direct  
98 observation of plastic debris in oceans is not yet possible via satellites since methods like remote  
99 sensing cannot observe small particles of plastic directly because of the instrument resolution.

100 Moreover, concentrations of microplastics are not high enough to modify the backscatter signal  
101 of the sea surface detectable by RADAR (used for monitoring hydrocarbon spills for instance).

102 In this study, we propose to correlate satellite observations with in situ microplastic  
103 concentrations.

104 During the sea campaign Expedition 7<sup>th</sup> Continent in June 2015, we performed in situ  
105 measurements while navigating around and across two individual cyclonic (CE) and  
106 anticyclonic eddies (AE) in the North Atlantic gyre. The localization of the eddies was  
107 beforehand determined by current forecasts. The aim of this study is to rationalize in situ  
108 microplastic surface concentrations with the altimetry data and model surface currents that are  
109 available globally at daily resolution.

## 110 **Materials and Methods**

### 111 **2015 North Atlantic sea campaign routing**

112 The sea campaign Expedition 7<sup>th</sup> Continent took place in the western North Atlantic subtropical  
113 gyre between 15 and 30°N and 55 and 65°W from 28<sup>th</sup> May to 16<sup>th</sup> June 2015 (Figure 1). The  
114 boat was guided day by day from Toulouse (France) using Copernicus Marine Environment  
115 Monitoring Service portal (CMEMS, <http://marine.copernicus.eu>). The forecasts were  
116 delivered by Mercator Ocean. The boat was guided day by day from Toulouse (France) thanks  
117 to CMEMS global ocean forecasts produced by Mercator Ocean. The CMEMS data was  
118 referenced as GLOBAL\_ANALYSIS\_FORECAST\_PHYS\_001\_002 (global ocean analysis  
119 and forecast model) and was available daily with a resolution of 1/12°. Our area of interest was  
120 mapped every day to forecast the following day's surface currents and sea surface height (SSH).  
121 In the area to be explored, SSH was between 3 and 40 cm and we planned to sample the whole  
122 range of SSH and to explore two mesoscale eddies. We tried to allocate sampling time evenly  
123 over the whole range of SSH but this was limited by logistical considerations, mainly the  
124 navigation speed and weather conditions.

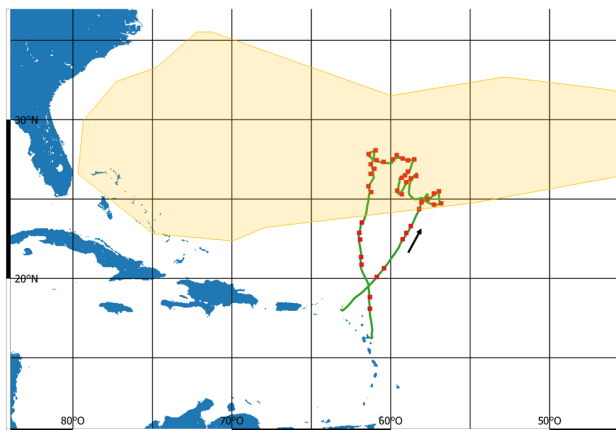
125

126

127 **Net tow sampling**

128 On the sailing vessel Guyavoile, net tows were conducted using Neuston nets with a standard  
129 mesh size of 300  $\mu\text{m}$ . Plastics were collected in a 0.5 m  $\times$  0.4 m rectangular frame fitted with a  
130 2 m long net. The net was equipped with a mechanical flow meter (Digital Flow Meter Model  
131 438 110, Hydro-bios, Altenholz Germany). The plastic debris was collected from the surface-  
132 layer at a depth of 0-20 cm. Tow durations were set to 30 min and were all undertaken while  
133 the vessel was travelling at a speed of 1 to 2.5 knots. The tows covered distances between 1.1  
134 to 2.5 km. The wind speed was measured with an anemometer fixed on top of the mast at 27 m.  
135 The Beaufort number was deduced from the wind speed measurements. The captain estimated  
136 the sea state of each sampling period. During this 17 day long campaign, 41 nets were towed.  
137 The date, GPS location, Beaufort number and sea state for each net tow is reported in table SI  
138 1.

139



140

141 Figure 1 : Map of subtropical North-Western Atlantic Ocean. The route of the boat is  
142 represented by the green line, the red squares mark the location of each net tow and the yellow  
143 shading corresponds to the plastic accumulation area according to Lebreton *et al.* (41).

144 **Microplastics sorting, counting, weighing and preservation**

145 On the boat, the contents of the tows were filtered on 300  $\mu\text{m}$  sieves. Most of the plastic debris  
146 was removed with tweezers and stored at  $-5^{\circ}\text{C}$  in glass vials. The remaining mixture of plankton  
147 and the smallest plastic debris was stored in flasks in a formol/sea water solution (5% vol  
148 formol) to preserve the plankton for identification and numbering. Under laboratory conditions  
149 and using a binocular microscope (magnification by 5 and 10), the small plastic debris was  
150 manually separated from natural matter with forceps. The remaining sample was inspected  
151 again on a glass plate. The plate was placed successively on top of white, black and red paper  
152 in order to sort out all the plastic debris. Sargassum was carefully inspected as plastic lines were  
153 often entangled in it. Microplastic is defined as plastic debris with a size below 5 mm (47). In  
154 this study, plastic debris were sampled using a mesh size of 300  $\mu\text{m}$ . All plastic debris was  
155 counted, including the mesoplastic (5 mm – 20 cm). Mesoplastics represented about 10% in  
156 number of the debris collected. Plastic pieces were arranged in 20 cm diameter glass petri dishes  
157 according to their size and color (Figure SI 1). Lines (the fibers were about one millimeter in  
158 diameter and were attributed to fishing lines because clothing fibers are typically thinner) were  
159 treated separately; they were measured manually with a ruler because they were often twisted.  
160 The petri dishes containing the pieces were scanned. The image was treated with ImageJ  
161 software. The pieces of plastic debris were individually identified and their length and width  
162 determined. Of the two dimensions established by ImageJ, the larger one was attributed to the  
163 length and the other to the width. All plastic debris were then weighed to the nearest 0.01 mg.  
164 Finally, they were stored individually in glass vials at  $-18^{\circ}\text{C}$  for further characterization. The  
165 uncorrected sea surface concentrations of microplastics ( $N_{\text{tow}}$ ) were expressed in number of  
166 pieces per square kilometer and are reported in Table SI 1.

### 167 **Surface concentrations correction**

168 The surface concentrations of microplastics were corrected in order to remove the variations  
169 induced by wind mixing ( $N$ ). We based our correction on the model described by Kukulka et



170 al. (48) and an adjustment of the plastic debris rising velocity from Reisser et al. (49). The detail  
171 of the correction is given in section SI 1 and values are reported in Table SI 1. Reisser et al.  
172 compared the correction model with in situ measurements between 0 and 5 m below the surface  
173 and observed a good correlation at Beaufort between 1 to 4. Hence, all stations at Beaufort 5  
174 were excluded from the discussion because the data were outside the limits of validity of the  
175 correction model. The mass concentrations were not corrected by the Kukulka model because  
176 the equations are based on the number of particles only.

### 177 **Sea Level Anomalies**

178 Sea level anomalies (SLA) are produced from satellite observations and, even if interpolation  
179 comes into play, these observations are much more precise than the SSH products from  
180 CMEMS used for routing the boat. Therefore SLA were used for the correlation with  
181 microplastic surface concentrations. We collected SLA observation products distributed by  
182 CMEMS portal and referenced as  
183 SEALEVEL\_GLO\_SLA\_MAP\_L4\_REP\_OBSERVATIONS\_008\_027. Data is produced by  
184 the Centre National d'Etudes Spatiales (CNES) in partnership with Collecte, Localisation,  
185 Satellites (CLS). Data is gridded and merged (interpolated from several satellites). Data is  
186 available daily and given with a formal mapping error of around 1 cm (depending on the  
187 location). The resolution is  $\frac{1}{4}^\circ$ . The SLA of the area explored were between -2.5 and 18 cm  
188 (details in Table SI 1). The SLA range was divided into three equal intervals: low (-2.5 to 5  
189 cm), medium (5 to 10 cm) and high (10 to 18 cm).

### 190 **Eddy identification**

191 Petersen et al.'s algorithm (50) was used to detect and track the mesoscale eddies in the sampled  
192 area using the Okubo-Weiss (OW) parameter. The OW parameter (W) is based on the velocity  
193 gradient tensor and highlights the flow part where vorticity dominates strain, which correspond  
194 to a negative parameter W. This parameter was calculated from surface current data available

195 from the CMEMS portal. This is a model product, referenced as  
196 GLOBAL\_ANALYSIS\_FORECAST\_PHYS\_001\_002. It is available daily with a resolution of  
197  $1/12^\circ$ . The algorithm made available on line by Petersen *et al.* (50) was used and was adapted  
198 to the format of the present data files (NetCDF).  $W$  can be calculated over the whole globe but  
199 this parameter needs a threshold depending on the region of the ocean to identify the eddy edge  
200 ( $\frac{W}{\sigma_W} \leq -0.2$  is usually used, where  $\sigma_W$  is the standard deviation of  $W$  over the region of interest)  
201 (50). We considered that translational motion of the eddy from east to west was negligible over  
202 the 15 days of the sampling period. We calculated the outlines of both eddies daily and defined  
203 their edges as the average over the 15 days.

#### 204 **Chlorophyll concentrations**

205 Chlorophyll-a (CHL-a) surface concentrations (in  $\text{mg}\cdot\text{m}^{-3}$ ) were obtained from the CMEMS  
206 portal (produced by ACRI-ST Company). They were near real time (NRT) observations  
207 referenced as OCEANCOLOUR\_GLO\_CHL\_L4\_NRT\_OBSERVATIONS\_009\_033. The  
208 data was based on images from the Moderate-Resolution Imaging Spectroradiometer (Modis)  
209 and Visible Infrared Imaging Radiometer Suite (Viirs) merged products. The daily data  
210 corresponded to a mesh of 4 km x 4 km ( $1/25^\circ$ ). The optimal interpolated L4 products were  
211 considered to avoid (interference from clouds).

#### 212 **Results and Discussion**

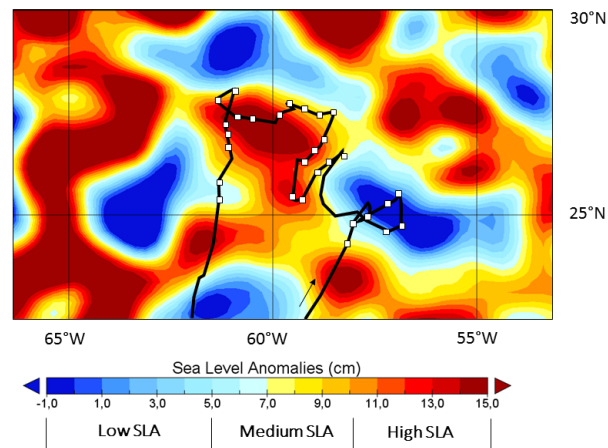
213 Microplastic surface concentrations will be either discussed uncorrected (Ntow expressed in  
214 pieces per square kilometer, Table SI 1), or corrected according to Kukulka model (N) (48).  
215 (48). The uncorrected data are available in the supporting material section and the corrected  
216 data are presented in the article; most studies present corrected data (37). Microplastic  
217 concentrations were typical of what is measured in the North Atlantic subtropical gyre  
218 (hundreds of thousands of pieces per square kilometer)(31).

219

220

### 221 **Correlation with Sea Level Anomalies**

222 During the sampling campaign, the explored area corresponded to SLA between -2.5 cm and  
223 +18 cm (Figure 2). This range was divided into three equal intervals.

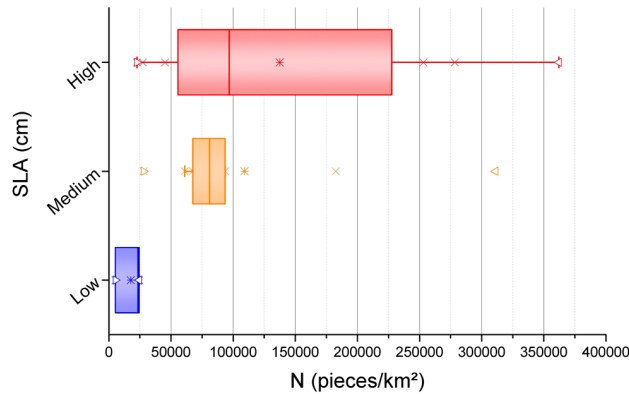


224

225 Figure 2: Map of the sampled area within the North Atlantic subtropical gyre correlated with  
226 Sea Level Anomalies satellite observations obtained from the CMEMS portal (on 1st June  
227 2015). The boat track is shown as a black line and was obtained by the Argos system; the  
228 sampling site locations are marked as white squares.

229 In total, we performed 41 measurements, 29 of which were within the subtropical gyre  
230 delimited by Lebreton et al. (41). On average, microplastic abundance concentrations were  
231 6.2 times higher inside the gyre than outside. In the subtropical gyre, microplastic corrected  
232 concentrations varied from 5,000 to 360,000 pieces/km<sup>2</sup>. The rest of the discussion concerns  
233 only the distribution of microplastics inside the subtropical gyre, where there were high  
234 variations (up to 70 fold). In spite of the dispersed values, N increased systematically with  
235 increasing SLA categories (Figure 3). The uncorrected correlation with SLA is given in figure  
236 SI 2 and show the same tendency. The statistical Mann Whitney test at 5% indicated that  
237 microplastic concentrations were significantly different at low and high SLA (mean N at low

238 SLA of 18000 pieces/km<sup>2</sup> and 138 000 pieces/km<sup>2</sup>. at high SLA, p=1.3%). Between these two  
 239 categories, the mean N differed by a factor of 7.7.  
 240

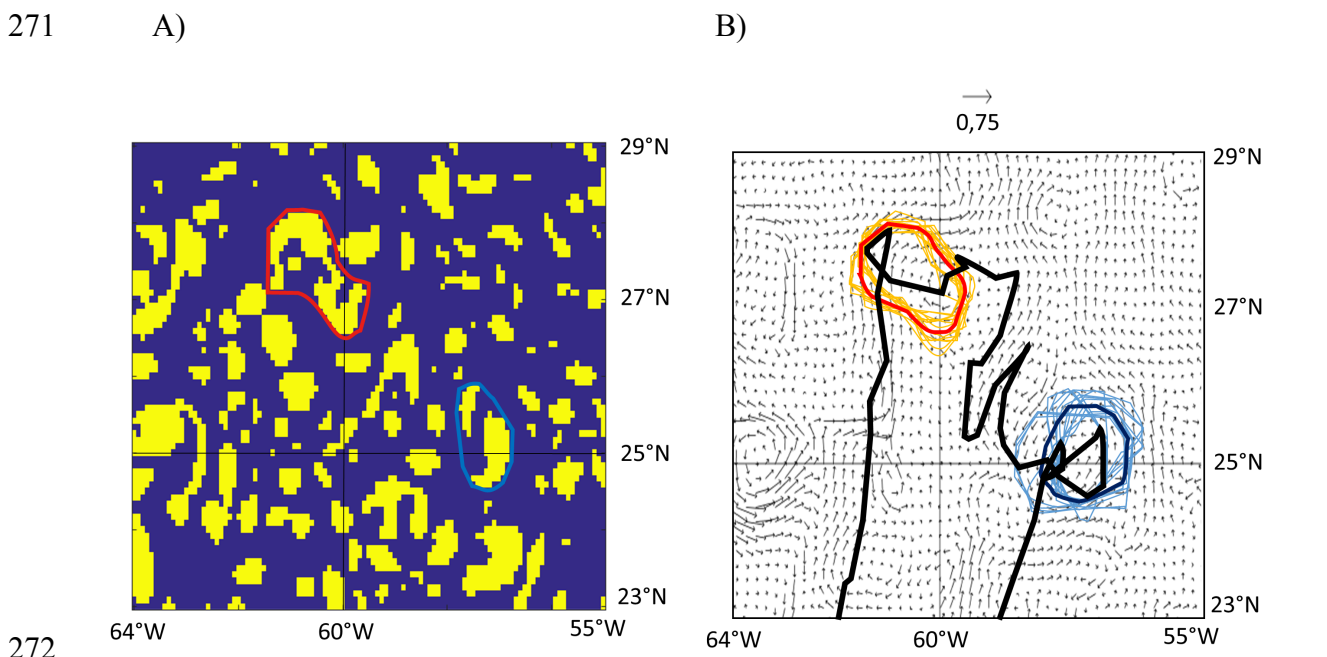


241  
 242  
 243  
 244 Figure 3: Corrected sea surface concentrations of microplastics (N, pieces/km<sup>2</sup>) according to  
 245 Sea Level Anomaly categories (SLA, cm). Whiskers correspond to 1.5 times the interquartile  
 246 range. Values are represented by crosses, min. and max. values by triangles, and mean values  
 247 by stars. This graph was obtained from 24 net tows (3 measurements at low SLA, 9 at medium  
 248 and 13 at high SLA).

249 **Correlation with model currents**

250 In addition to investigating the correlation between the distribution of microplastics and SLA,  
 251 the variations in local ocean circulation and particularly mesoscale eddies will be discussed.  
 252 Eddies are coherent mesoscale vortices of water that play a key role in the ocean. They have a  
 253 dynamic influence in the ocean, especially on the transport of heat, salt, and water masses. They  
 254 also have a biological influence through upwelling of cold water rich in nutrients for the growth  
 255 of phytoplankton or, on the contrary, downwelling (depending on the sense of rotation).  
 256 There are various methods to identify eddies and determine their contour, using SLA is a first  
 257 one, where the eddy boundaries are set to SLA above a given threshold (51, 52). There are also  
 258 methods based on the Okubo-Weiss (OW) parameter using velocity fields under vorticity-  
 259 dominated flows. We used this parameter and, as described in Figure 5, the two eddies explored

260 had well defined boundaries, which were determined by taking the average of the outlines found  
 261 over 15 consecutive days. A movie showing the OW parameter over the 15 days of sampling is  
 262 available in SI (Movie SI 1). Peterson et al. used a minimum lifetime cutoff of 28 days for well-  
 263 defined eddies (50). We ensured indeed that the two eddies explored had a lifetime well above  
 264 that limit, they indeed already existed 6 months earlier (Figure SI 3). In June 2015, the cyclonic  
 265 eddy was approximately 200 km by 150 km and the anticyclonic eddy was 200 km by 100 km.  
 266 The centers of their ellipsoids were about 400 km apart and, edge to edge, they were around  
 267 200 km apart. It took 5 days with to sail from one eddy to the other in bad weather conditions.  
 268 As expected, the eddy edges were correlated with SLA values (see Figure SI 4) even though  
 269 there was not a perfect match. This was principally due to a difference in resolution between  
 270 the two data sets.

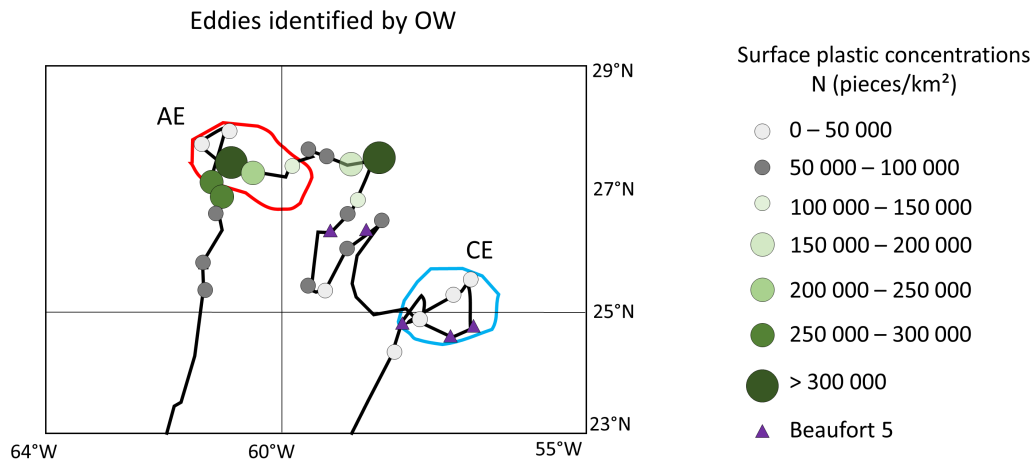


274 Figure 5: A) Example of daily Okubo-Weiss parameter calculated using surface currents data  
 275 from the CMEMS portal (data from 14th June 2015). The yellow areas correspond to an OW  
 276 parameter that is negative with respect to a flow dominated by vorticity. The anticyclonic and  
 277 cyclonic eddies boundaries explored are represented by red and blue lines respectively. B) Map  
 278 representing the mean surface current vectors between 1st and 15th June 2015, the boat track

279 of the 7<sup>th</sup> Continent expedition is reported as a black line. The daily calculated eddy boundaries  
280 are represented by thin lines. In bold line was represented the average of the outlines calculated  
281 over 15 consecutive days. As the translational east-west motion of eddies was negligible over  
282 this time period, their boundaries were defined as the mean (bold line).

283 Microplastic surface concentrations were then compared within the two eddies (Figure 6, for  
284 uncorrected data see Figure SI 5). The mean N value in the cyclonic eddy was 20,000  
285 pieces/km<sup>2</sup> compared to 170,000 pieces/km<sup>2</sup> in the anticyclonic eddy. The averaged  
286 microplastic surface concentration was 9.4 higher in the anticyclonic eddy. There is an  
287 important plastic concentration at the south east of the AE (Figure 6), it is just at the limit of its  
288 boundaries and it illustrates the uncertainties of the mathematic delimitation of eddies edges.  
289 This measurement could have been included in the calculation of the ratio AE/CE that would  
290 then equal 10.3 . There was also significant plastic debris concentrations at the east of the AE,  
291 it was located between two AE as can be seen in figure 2. There are very complicated turbulent  
292 effects at the eddies edges, convergence and divergence at small scale features could occur and  
293 influence plastic distribution at the surface. It would be very interesting to study these  
294 phenomenon in the future. In summary, from our in situ measurements, we observe that the  
295 anticyclonic eddy tended to accumulate more floating microplastic than the cyclonic eddy.

296 New figure 6



297

298 **Figure 6: Corrected surface microplastic concentrations (N) inside the gyre correlated with**  
 299 **delimitation of eddies calculated using the Okubo-Weiss (OW) parameter. The route taken by**  
 300 **the boat is shown as a black line, eddy boundaries are marked in blue and red for the cyclonic**  
 301 **(3 measurements) and anticyclonic eddies (6 measurements), respectively.**

302 Mesoscale eddies contribute to horizontal and vertical nutrient fluxes within the euphotic zone  
 303 (44). They cause nutrient-rich water to upwell by various mechanisms, thus stimulating the  
 304 growth of phytoplankton and increasing the amount of chlorophyll in the eddy core (53-56).  
 305 CHL-a surface concentrations from satellite observations were compared between the two  
 306 eddies on a daily basis in order to eliminate the variations induced by local parameters (e.g.  
 307 temperature, sunshine). The two eddies were close enough (around 200 km apart edge to edge)  
 308 to make this comparison possible. Daily CHL-a surface concentrations were averaged over the  
 309 entire area of the eddy. Over the sampling period, CHL-a mean surface concentrations were, on  
 310 average, 30% higher in the anticyclonic eddy than in the cyclonic eddy (see table SI 2 for  
 311 details).

312 In conclusion, this study presents the first direct observation of different concentrations of  
 313 plastic between a cyclonic and an anticyclonic mesoscale eddy. Although the sample size is  
 314 small, the results here corroborate the hypothesis that mesoscale ocean dynamics impact plastic  
 315 debris distribution at the sea surface within subtropical gyres. We strongly encourage further

316 analysis of this effect in other trawl datasets. As anticyclonic eddies also tend to trap and  
317 transport nutrients, chlorophyll and zooplankton, the environmental impact of plastic pollution  
318 should be considered from this perspective. Real-time surveys of the sea surface by space based  
319 instruments may therefore help to plan future campaigns with respect to the mesoscale  
320 convergence in eddies. Vortices in turbulence are often envisaged as rotating bodies of fluid,  
321 traveling as coherent islands in an incoherent ambient flow (45, 57) and it would be interesting  
322 to estimate the proportion of debris gathered and entrapped from the early stage of the eddy  
323 existence and the proportion of material captured and swallowed as the eddy travels east-west  
324 inside the gyre. Of course, the leakage of material from eddies must also be considered. Finally,  
325 this study has only considered microplastics at the sea surface and the investigation of  
326 microplastics throughout the water column needs to be undertaken. As anticyclones are  
327 generally downwelling, how abundant would microplastic be at greater depths, especially at the  
328 core of eddies where the geostrophic speed is locally maximum at a certain depth (58)?  
329  
330



331 **Acknowledgments**

332 We thank the NGO Expedition 7<sup>th</sup> Continent for the logistic of the sea campaign and the NGO  
333 Ocean Science Logistic for building the manta nets. This research was funded by the CNES and  
334 by the Total foundation. EvS was supported through funding from the European Research  
335 Council (ERC) under the European Union's Horizon 2020 research and innovation programme  
336 (grant agreement No 715386).

337

338 **References**

- 339 1. Zylstra ER (2013) Accumulation of wind-dispersed trash in desert environments. *J Arid*  
340 *Environ* 89:13-15.
- 341 2. Bakir A, Rowland SJ, & Thompson RC (2014) Transport of persistent organic  
342 pollutants by microplastics in estuarine conditions. *Estuar Coast Shelf S* 140:14-21.
- 343 3. McCormick A, Hoellein TJ, Mason SA, Schlupe J, & Kelly JJ (2014) Microplastic is  
344 an Abundant and Distinct Microbial Habitat in an Urban River. *Environ Sci Technol*  
345 48(20):11863-11871.
- 346 4. Faure F, Demars C, Wieser O, Kunz M, & de Alencastro LF (2015) Plastic pollution in  
347 Swiss surface waters: nature and concentrations, interaction with pollutants. *Environ*  
348 *Chem* 12(5):582-591.
- 349 5. Eriksen M, Mason S, Wilson S, Box C, Zellers A, Edwards W, Farley H, & Amato S  
350 (2013) Microplastic pollution in the surface waters of the Laurentian Great Lakes. *Mar*  
351 *Pollut Bull* 77(1-2):177-182.
- 352 6. Schlining K, von Thun S, Kuhnz L, Schlining B, Lundsten L, Stout NJ, Chaney L, &  
353 Connor J (2013) Debris in the deep: Using a 22-year video annotation database to survey  
354 marine litter in Monterey Canyon, central California, USA. *Deep Sea Res Part 1*  
355 *Oceanogr Res Pap* 79:96-105.
- 356 7. Phillips MB & Bonner TH (2015) Occurrence and amount of microplastic ingested by  
357 fishes in watersheds of the Gulf of Mexico. *Mar Pollut Bull* 100(1):264-269.
- 358 8. Eriksen M, Lebreton LCM, Carson HS, Thiel M, Moore CJ, Borerro JC, Galgani F,  
359 Ryan PG, & Reisser J (2014) Plastic Pollution in the World's Oceans: More than 5  
360 Trillion Plastic Pieces Weighing over 250,000 Tons Afloat at Sea. *PLoS ONE* 9(12).
- 361 9. Jambeck JR, Geyer R, Wilcox C, Siegler TR, Perryman M, Andrady A, Narayan R, &  
362 Law KL (2015) Plastic waste inputs from land into the ocean. *Science* 347(6223):768-  
363 771.
- 364 10. Moore CJ (2008) Synthetic polymers in the marine environment: A rapidly increasing,  
365 long-term threat. *Environ Res* 108(2):131-139.
- 366 11. ter Halle A, Ladirat L, Gendre X, Goudouneche D, Pusineri C, Routaboul C, Tenailleau  
367 C, Duployer B, & Perez E (2016) Understanding the Fragmentation Pattern of Marine  
368 Plastic Debris. *Environ Sci Technol* 50(11):5668-5675.
- 369 12. Gigault J, Pedrono B, Maxit B, & Ter Halle A (2016) Marine plastic litter: the  
370 unanalyzed nano-fraction. *Environ Sci-Nano* 3(2):346-350.

- 371 13. Lusher AL, McHugh M, & Thompson RC (2013) Occurrence of microplastics in the  
372 gastrointestinal tract of pelagic and demersal fish from the English Channel. *Mar Pollut*  
373 *Bull* 67(1-2):94-99.
- 374 14. Lusher AL, Hernandez-Millan G, O'Brien J, & Berrow S (2015) Microplastic and  
375 macroplastic ingestion by a deep diving, oceanic cetacean: The true's beaked whale  
376 *Mesoplodon mirus*. *Environ Pollut* 199:185-191.
- 377 15. Schuyler Q, Hardesty BD, Wilcox C, & Townsend K (2012) To Eat or Not to Eat?  
378 Debris Selectivity by Marine Turtles. *PLoS ONE* 7(7).
- 379 16. English MD, Robertson GJ, Avery-Gomm S, Pine-Hay D, Roul S, Ryan PC, Wilhelm  
380 SI, & Mallory ML (2015) Plastic and metal ingestion in three species of coastal  
381 waterfowl wintering in Atlantic Canada. *Mar Pollut Bull* 98(1-2):349-353.
- 382 17. Ryan PG (2015) How quickly do albatrosses and petrels digest plastic particles? *Environ*  
383 *Pollut* 207:438-440.
- 384 18. Wilcox C, Van Sebille E, & Hardesty BD (2015) Threat of plastic pollution to seabirds  
385 is global, pervasive, and increasing. *Proc Natl Acad Sci USA* 112(38):11899-11904.
- 386 19. Collard F, Gilbert B, Eppe G, Parmentier E, & Das K (2015) Detection of  
387 Anthropogenic Particles in Fish Stomachs: An Isolation Method Adapted to  
388 Identification by Raman Spectroscopy. *Arch Environ Con Tox* 69(3):331-339.
- 389 20. Cole M, Lindeque P, Fileman E, Halsband C, Goodhead R, Moger J, & Galloway TS  
390 (2013) Microplastic Ingestion by Zooplankton. *Environ Sci Technol* 47(12):6646-6655.
- 391 21. Cole M & Galloway TS (2015) Ingestion of Nanoplastics and Microplastics by Pacific  
392 Oyster Larvae. *Environ Sci Technol* 49(24):14625-14632.
- 393 22. Cole M, Lindeque P, Fileman E, Halsband C, & Galloway TS (2015) The Impact of  
394 Polystyrene Microplastics on Feeding, Function and Fecundity in the Marine Copepod  
395 *Calanus helgolandicus*. *Environ Sci Technol* 49(2):1130-1137.
- 396 23. Goldstein MC, Carson HS, & Eriksen M (2014) Relationship of diversity and habitat  
397 area in North Pacific plastic-associated rafting communities. *Mar Biol* 161(6):1441-  
398 1453.
- 399 24. Zettler ER, Mincer TJ, & Amaral-Zettler LA (2013) Life in the "Plastisphere":  
400 Microbial Communities on Plastic Marine Debris. *Environ Sci Technol* 47(13):7137-  
401 7146.
- 402 25. Rochman CM, Browne MA, Halpern BS, Hentschel BT, Hoh E, Karapanagioti HK,  
403 Rios-Mendoza LM, Takada H, Teh S, & Thompson RC (2013) Classify plastic waste  
404 as hazardous. *Nature* 494(7436):169-171.
- 405 26. Rochman CM, Lewison RL, Eriksen M, Allen H, Cook AM, & Teh SJ (2014)  
406 Polybrominated diphenyl ethers (PBDEs) in fish tissue may be an indicator of plastic  
407 contamination in marine habitats. *Sci Total Environ* 476:622-633.
- 408 27. Rochman CM, Kurobe T, Flores I, & Teh SJ (2014) Early warning signs of endocrine  
409 disruption in adult fish from the ingestion of polyethylene with and without sorbed  
410 chemical pollutants from the marine environment. *Sci Total Environ* 493:656-661.
- 411 28. Rochman CM, Hoh E, Kurobe T, & Teh SJ (2013) Ingested plastic transfers hazardous  
412 chemicals to fish and induces hepatic stress. *Scientific Reports* 3.
- 413 29. Tanaka K, Takada H, Yamashita R, Mizukawa K, Fukuwaka M, & Watanuki Y (2013)  
414 Accumulation of plastic-derived chemicals in tissues of seabirds ingesting marine  
415 plastics. *Mar Pollut Bull* 69(1-2):219-222.
- 416 30. Wardrop P, Shimeta J, Nugegoda D, Morrison PD, Miranda A, Tang M, & Clarke BO  
417 (2016) Chemical Pollutants Sorbed to Ingested Microbeads from Personal Care  
418 Products Accumulate in Fish. *Environ Sci Technol* 50(7):4037-4044.

- 419 31. Law KL, Moret-Ferguson S, Maximenko NA, Proskurowski G, Peacock EE, Hafner J,  
420 & Reddy CM (2010) Plastic Accumulation in the North Atlantic Subtropical Gyre.  
421 *Science* 329(5996):1185-1188.
- 422 32. Eriksen M, Maximenko N, Thiel M, Cummins A, Lattin G, Wilson S, Hafner J, Zellers  
423 A, & Rifman S (2013) Plastic pollution in the South Pacific subtropical gyre. *Mar Pollut*  
424 *Bull* 68(1-2):71-76.
- 425 33. Goldstein MC, Titmus AJ, & Ford M (2013) Scales of Spatial Heterogeneity of Plastic  
426 Marine Debris in the Northeast Pacific Ocean. *PLoS ONE* 8(11).
- 427 34. Van Sebille E (2015) The oceans' accumulating plastic garbage. *Physics today* 68(2):60-  
428 61.
- 429 35. Moret-Ferguson S, Law KL, Proskurowski G, Murphy EK, Peacock EE, & Reddy CM  
430 (2010) The size, mass, and composition of plastic debris in the western North Atlantic  
431 Ocean. *Mar Pollut Bull* 60(10):1873-1878.
- 432 36. Law KL, Moret-Ferguson SE, Goodwin DS, Zettler ER, De Force E, Kukulka T, &  
433 Proskurowski G (2014) Distribution of Surface Plastic Debris in the Eastern Pacific  
434 Ocean from an 11-Year Data Set. *Environ Sci Technol* 48(9):4732-4738.
- 435 37. Cozar A, Echevarria F, Gonzalez-Gordillo JI, Irigoien X, Ubeda B, Hernandez-Leon S,  
436 Palma AT, Navarro S, Garcia-de-Lomas J, Ruiz A, Fernandez-de-Puelles ML, & Duarte  
437 CM (2014) Plastic debris in the open ocean. *Proc Natl Acad Sci USA* 111(28):10239-  
438 10244.
- 439 38. van Sebille E, Wilcox C, Lebreton L, Maximenko N, Hardesty BD, van Franeker JA,  
440 Eriksen M, Siegel D, Galgani F, & Law KL (2015) A global inventory of small floating  
441 plastic debris. *Environ Res Lett* 10(12).
- 442 39. Froyland G, Stuart RM, & van Sebille E (2014) How well-connected is the surface of  
443 the global ocean? *Chaos* 24(3).
- 444 40. Maximenko N, Hafner J, & Niiler P (2012) Pathways of marine debris derived from  
445 trajectories of Lagrangian drifters. *Mar Pollut Bull* 65(1-3):51-62.
- 446 41. Lebreton LCM, Greer SD, & Borrero JC (2012) Numerical modelling of floating debris  
447 in the world's oceans. *Mar Pollut Bull* 64(3):653-661.
- 448 42. Flierl GR (1981) Particle Motions in Large-Amplitude Wave Fields. *Geophys Astro*  
449 *Fluid* 18(1-2):39-74.
- 450 43. Early JJ, Samelson RM, & Chelton DB (2011) The Evolution and Propagation of  
451 Quasigeostrophic Ocean Eddies. *J Phys Oceanogr* 41(8):1535-1555.
- 452 44. Chelton DB, Gaube P, Schlax MG, Early JJ, & Samelson RM (2011) The Influence of  
453 Nonlinear Mesoscale Eddies on Near-Surface Oceanic Chlorophyll. *Science*  
454 334(6054):328-332.
- 455 45. Haller G & Beron-Vera FJ (2013) Coherent Lagrangian vortices: the black holes of  
456 turbulence. *J Fluid Mech* 731.
- 457 46. Beron-Vera FJ, Olascoaga MJ, & Lumpkin R (2016) Inertia-induced accumulation of  
458 flotsam in the subtropical gyres. *Geophys Res Lett*.
- 459 47. Arthur C, Baker J, & Bamford H (2009) Proceedings of the international research  
460 workshop on the occurrence, effects, and fate of microplastic marine debris ed Program  
461 NMD.
- 462 48. Kukulka T, Proskurowski G, Moret-Ferguson S, Meyer DW, & Law KL (2012) The  
463 effect of wind mixing on the vertical distribution of buoyant plastic debris. *Geophys Res*  
464 *Lett* 39.
- 465 49. Reisser J, Slat B, Noble K, du Plessis K, Epp M, Proietti M, de Sonnevile J, Becker T,  
466 & Pattiaratchi C (2015) The vertical distribution of buoyant plastics at sea: an observational  
467 study in the North Atlantic Gyre. *Biogeosciences* 12:1249-1256.

- 468 50. Petersen MR, Williams SJ, Maltrud ME, Hecht MW, & Hamann B (2013) A three-  
469 dimensional eddy census of a high-resolution global ocean simulation. *J Geophys Res-*  
470 *Oceans* 118(4):1759-1774.
- 471 51. Fang FX & Morrow R (2003) Evolution, movement and decay of warm-core Leeuwin  
472 Current eddies. *Deep-Sea Res Pt II* 50(12-13):2245-2261.
- 473 52. Chaigneau A & Pizarro O (2005) Eddy characteristics in the eastern South Pacific. *J*  
474 *Geophys Res-Oceans* 110(C6).
- 475 53. Falkowski PG, Ziemann D, Kolber Z, & Bienfang PK (1991) Role of Eddy Pumping in  
476 Enhancing Primary Production in the Ocean. *Nature* 352(6330):55-58.
- 477 54. McNeil JD, Jannasch HW, Dickey T, McGillicuddy D, Brzezinski M, & Sakamoto CM  
478 (1999) New chemical, bio-optical and physical observations of upper ocean response to  
479 the passage of a mesoscale eddy off Bermuda. *J Geophys Res-Oceans* 104(C7):15537-  
480 15548.
- 481 55. McGillicuddy DJ, Johnson R, Siegel DA, Michaels AF, Bates NR, & Knap AH (1999)  
482 Mesoscale variations of biogeochemical properties in the Sargasso Sea. *J Geophys Res-*  
483 *Oceans* 104(C6):13381-13394.
- 484 56. Siegel DA, McGillicuddy DJ, & Fields EA (1999) Mesoscale eddies, satellite altimetry,  
485 and new production in the Sargasso Sea. *J Geophys Res-Oceans* 104(C6):13359-13379.
- 486 57. Froyland G, Horenkamp C, Rossi V, & van Sebille E (2015) Studying an Agulhas ring's  
487 long-term pathway and decay with finite-time coherent sets. *Chaos* 25(8).
- 488 58. Chaigneau A, Le Texier M, Eldin G, Grados C, & Pizarro O (2011) Vertical structure  
489 of mesoscale eddies in the eastern South Pacific Ocean: A composite analysis from  
490 altimetry and Argo profiling floats. *J Geophys Res-Oceans* 116.

491

492